Contrasting the synoptic drivers of the UK heatwaves of 1976, 2003, 2018 and 2022

Sladić, N. ORCID: https://orcid.org/0000-0001-5170-1374, Allan, R. P. ORCID: https://orcid.org/0000-0003-0264-9447, Trent, T. ORCID: https://orcid.org/0000-0001-9215-5808, Povey, A. C. ORCID: https://orcid.org/0000-0002-4109-9639 and Suri, D. ORCID: https://orcid.org/0009-0003-1354-7873
(2026) Contrasting the synoptic drivers of the UK heatwaves of 1976, 2003, 2018 and 2022. Weather. ISSN 1477-8696 doi: 10.1002/wea.70075 Available at https://centaur.reading.ac.uk/129705/

Contrasting the synoptic drivers of the UK heatwaves of 1976, 2003, 2018 and 2022

Nedim Sladić[1,2], Richard P. Allan[2], Tim Trent[1], Adam C. Povey[1] and Dan Suri[3]

[1]*School of Physics and Astronomy/ National Centre for Earth Observation, University of Leicester, UK*
[2]*Department of Meteorology, National Centre for Earth Observation, University of Reading, UK*
[3]*Met Office, Exeter, UK*

Introduction

In a warming climate, heatwaves are becoming one of the most overlooked issues for global societies, posing significant health risks to all population groups (Stott *et al.*, 2004; Brimicombe *et al.*, 2021). With rising temperatures, the window for more frequent and intense heatwaves widens, and events such as in the UK in 2018 are now estimated to be 30 times more likely under human-induced climate change (Lowe *et al.*, 2019; Christidis *et al.*, 2020). Heat-related deaths also increase with the higher number of hot days; heatwaves in 2003 and 2022 (Black *et al.*, 2004; Luterbacher *et al.*, 2004; Schär *et al.*, 2004; Stott *et al.*, 2004; Ballester *et al.*, 2023) led to the loss of 2139 and 4508 lives, respectively (Johnson *et al.*, 2005; Office for National Statistics and UK Health Security Agency, 2023). With mean UK summer temperatures set to be 5°C higher by 2070 (Sahani *et al.*, 2022), projections estimate up to 7000 heat-related deaths in the UK annually by 2050 (Howarth *et al.*, 2019; Brimicombe *et al.*, 2021; Dickinson *et al.*, 2025), stressing the need for the UK's National Health Service to protect vulnerable population groups from the adverse heat-related risks.

However, not all heatwaves result in excess mortality or infrastructural damage; each possess distinct patterns and spatiotemporal characteristics influenced by feedback mechanisms (Fischer *et al.*, 2007; Pfahl and Wernli, 2012). Across the midlatitudes, summer heatwaves often arise from persistent, slow-moving (or blocked) high-pressure systems weakening the zonal flow and enhancing subsidence and adiabatic air compression, heating the air within the planetary boundary layer (Stefanon *et al.* 2012; Zschenderlein *et al.*, 2019). Such sinking motion suppresses cloud development, reduces precipitation and depletes soil moisture, resulting in solar radiation largely heating the ground rather than evaporating water (e.g. Tyrlis and Hoskins, 2008; Stefanon *et al.* 2012; Mann *et al.*, 2017; Rouges *et al.*, 2023). A stalling blocking weather regime over Fennoscandia can lead to easterly and southeasterly air streams transporting hot, dry continental air from mainland Europe to the UK with a limited moistening source. While the central Atlantic low-pressure system imports hot tropical continental air mass from Iberia, forcing southerly and southwesterly flow that arches the jet stream poleward (Cassou *et al.*, 2005; Zschenderlein *et al.*, 2019). Both blocking and the Atlantic low regime are associated with positive zonal wind anomalies and sharper upper-level potential vorticity gradients. This forces upper-level ageostrophic divergence and ascent, favouring more intense weather systems. Both regimes are associated with a higher number of hot days, especially if preceded by three dry months (Quesada *et al.*, 2012). However, the mechanisms remain unclear due to their thermodynamic complexity (Strigunova *et al.*, 2022).

The double jet stream has also been linked to enhanced heatwaves in western Europe, notably in 1976, 2003 and 2018, due to an anomalous decrease in zonal winds at 200hPa (Rousi *et al.*, 2022). This change reinforces the easterly flow and persistent blocking signals, where behaviour of Rossby waves alters atmospheric flow variance in mid-latitudes and the Arctic (Rudeva and Simmonds, 2021; Luo *et al.*, 2024). The slow

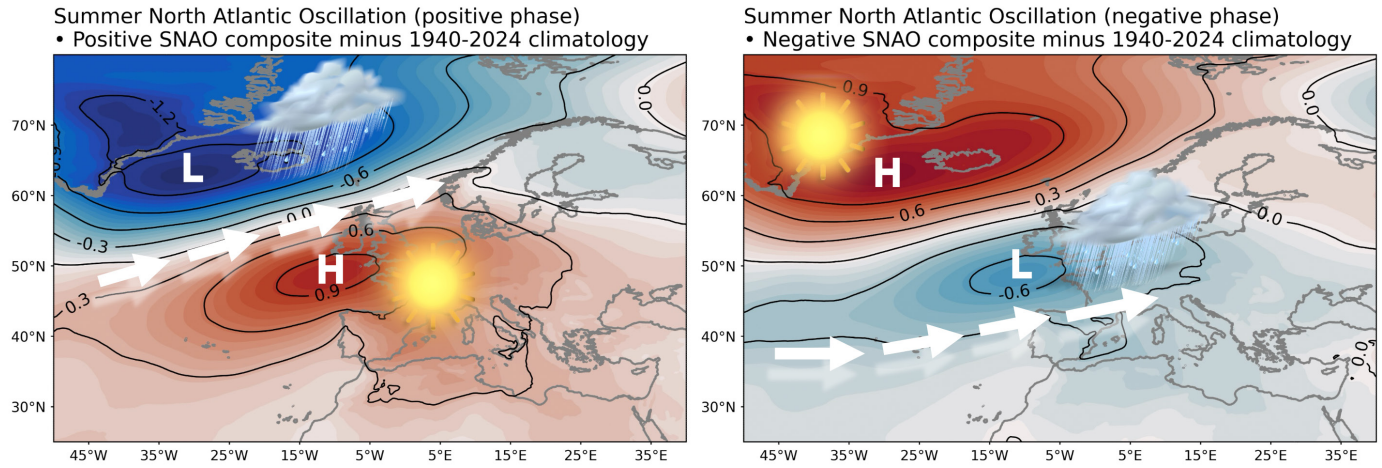

Figure 1. Illustration of the positive (left) and negative (right) SNAO phases, computed as the composite of all filtered summers (i.e. JJA) between 1940 and 2024 from the NCEP/NCAR dataset: mean JJA values greater or below 0.1 are ascribed to positive and negative indices, respectively, without any classification performed. Then, the 1940–2024 ERA5 reanalysis JJA mean sea-level pressure climatology provides the pressure anomalies (contours and shading at 0.3 interval), with the dominant weather conditions and mean jet stream position indicated by the corresponding icons and arrows, respectively.

propagation and persistence of these planetary waves contribute to extreme weather conditions (Coumou *et al*., 2018). Recent hot summers (i.e. 2003, 2006, 2018) have additionally been attributed to an amplification of planetary wavenumber 7, corresponding to recurrent heatwave patterns across western Europe (Kornhuber *et al*., 2019).

Positive land-atmosphere feedback, particularly in soil moisture, can also play a significant role in heatwave amplification, especially after dry periods (Black *et al*., 2004; Fischer *et al*., 2007; Alexander, 2011; Hirschi *et al*., 2011; Miralles *et al*., 2014, 2019; Zschenderlein *et al*., 2019). Additionally, the warmer sea surface temperatures (SSTs) in the Mediterranean during summer 2022 contributed to precipitation suppression in western Europe and increased surface heating, driven by atmospheric forcing (Guinaldo *et al*., 2023). The occurrence of the tripole pattern in the North Atlantic, with warmer-than-normal SSTs in the central portion, and cooler temperatures towards the Azores to the south and Newfoundland to the north, can also coincide with the polar jet being north of the UK (Dunstone *et al*., 2019; McCarthy *et al*., 2019), and reflects behaviour typical of a positive Summer North Atlantic Oscillation (SNAO+) index (Figure 1).

In this study, the summers of 1976, 2003, 2018 and 2022 are analysed to understand the key factors behind heatwaves in the UK. The 1976 and 2018 cases focus on high-pressure system blocking signatures influenced by the SNAO+ phase (e.g. Dunstone *et al*., 2019; McCarthy *et al*., 2019), while 2003 and 2022 are identified for their record-breaking temperatures (e.g. Black *et al*., 2004; Yule *et al*., 2023). The research aims to address the following questions:

1. How do atmospheric teleconnection patterns influence temperatures and precipitation in the UK?
2. What synoptic conditions favour heatwave development in the UK?
3. How can heatwaves be enhanced through land-atmosphere and ocean–atmosphere coupling?
4. Which weather regimes support UK heatwaves?

Table 1

Summary of all datasets leveraged to conduct the research (Barnston and Livezey, 1987; Parker et al., 1992; Alexander and Jones, 2000; Neal et al., 2016; Hersbach et al., 2020; Neal, 2022).

Dataset	*Dataset type*	*Variables considered*	*Identified strengths*	*Identified weaknesses*
ERA5	Reanalysis	Zonal wind at 200hPa, geopotential height at 500hPa, mean sea-level pressure, soil moisture at 0–7cm level, sea surface temperatures	On par with the observational E-OBS surface dataset for the extremely high temperatures ($r = 0.995$), low RMSE (0.52°C), statistical and standard deviation biases (0.23°C and 0.47°C, respectively) (Mistry *et al*., 2022; Velikou *et al*., 2022). Compensates for the lack of surface variables (e.g. soil moisture) and upper-tropospheric (vertical profile) variables (e.g. geopotential height, mean wind speed, temperature, etc.)	Influenced by the data availability from the past, affecting the reanalysis constancy (Bell *et al*., 2021), model biases (Cucchi *et al*., 2020) and changing observing systems through time related to the data incorporation from the buoys, satellites and weather stations used for the data assimilation (Hersbach *et al*., 2020; Bell *et al*., 2021)
NCEP/NCAR	Instrumental and precomputed	Gyre differences between Reykjavik and Gibraltar – SNAO index; difference between the high-pressure gyre over Fennoscandia and an attenuated low-pressure gyre over Western Mongolia or Eastern Russia (Barnston and Livezey, 1987) – SCAN index	Strict and robust measurement control; reliance on the principal component indices data recalculation of the empirical orthogonal function and its spatial patterns representation	Loss of data (Jones *et al*., 1997) and limited timespan
HadCET	Observational	Central England Temperature (CET)	Rigorous observed data control and 99% diagnosed accuracy, up to 0.1°C (Parker and Horton, 2005), and correction to the urban warming (1974 onwards) with an adjustment of up to 0.2°C applied to mean temperature	Triangular extent (i.e. London–Bristol–Lancashire triangular area) of the HadCET does not consider the surface observations outside the region
HadUKP	Observational	Central England Precipitation (CEP)	The longest (1766–present) and, to date, the most accurate regional dataset available for England and Wales/Cymru (Alexander and Jones, 2000)	–
MO-30	Climatology	UK Met Office weather regimes	Provides frequency with which common specific weather patterns occur across the UK (Ansell *et al*., 2006; Neal *et al*., 2016; Neal, 2022); links to the potential relationship to large-scale drivers and fortifies the findings in the heatwave development across the British Isles	–

Datasets

Reanalysis dataset

The key prognostic variables (zonal winds at 200hPa, geopotential height at 500hPa, mean sea-level pressure, soil moisture at 0–7cm level and SSTs) are leveraged to evaluate the heatwave evolution and amplification factors for the selected test cases across the British Isles using ERA5 reanalysis data (Hersbach *et al*., 2020). The anomalies are calculated relative to the 1961–1990 reference period, spanning meteorological summer (i.e. June–July–August, JJA) and highlighting more the weather pattern signature rather than climate warming signals.

Precomputed and instrumental datasets

The NCEP/NCAR instrumental and precomputed datasets are selected for the large-scale atmospheric drivers – the SNAO (Hurrell, 1995; Jones *et al*., 1997) and Fennoscandian index (SCAN), previously known as Eurasia-1 pattern (Barnston and Livezey, 1987) – spanning the meteorological summer season.

The SNAO explains the spatial strength variability during the boreal summer between the low-pressure system near Iceland and high-pressure system north of the Azores. It is responsible for determining the storm tracks across northwestern Europe, modulating the precipitation, temperature and cloudiness over the region (Folland *et al*., 2009).

The SCAN describes the primary air circulation over Fennoscandia, while the compensatory attenuated low-pressure centres are situated either across Eastern Russia or Western Mongolia, or over western Europe (Barnston and Livezey, 1987).

Observational datasets

The mean monthly air temperature and accumulated precipitation are taken from the UK Met Office HadCET (Parker *et al*., 1992) and HadUKP datasets (Alexander and Jones, 2000). HadCET is the longest available temperature time series dataset (1659–present) and comprises the observational data collected in a roughly triangular area between London, Bristol and Lancashire. The HadUKP (Alexander and Jones, 2000) incorporates the longest (1766–present) and most accurate regional dataset representation available for England and Wales (Cymru) to-date.

Climatology dataset

Furthermore, to link the potential relationship to large-scale drivers and fortify the findings in the heatwave development across the British Isles, the 30 weather patterns defined for the UK are considered using MO-30 (Ansell *et al*., 2006; Neal *et al*., 2016; Neal, 2022). These regimes are based on the classification frequency of specific localised weather regimes in the UK throughout the year.

Table 1 summarises the each of the datasets, highlighting their strengths and weaknesses.

Methods

The antecedent and synoptic conditions are averaged, with anomalies calculated with respect to the 1961–1990 reference period to highlight the warming signal. Similarly, the HadCET and HadCEP datasets are summed and averaged over the JJA period, then compared with the reference climatology to establish the trend across the UK and tested against the SNAO and

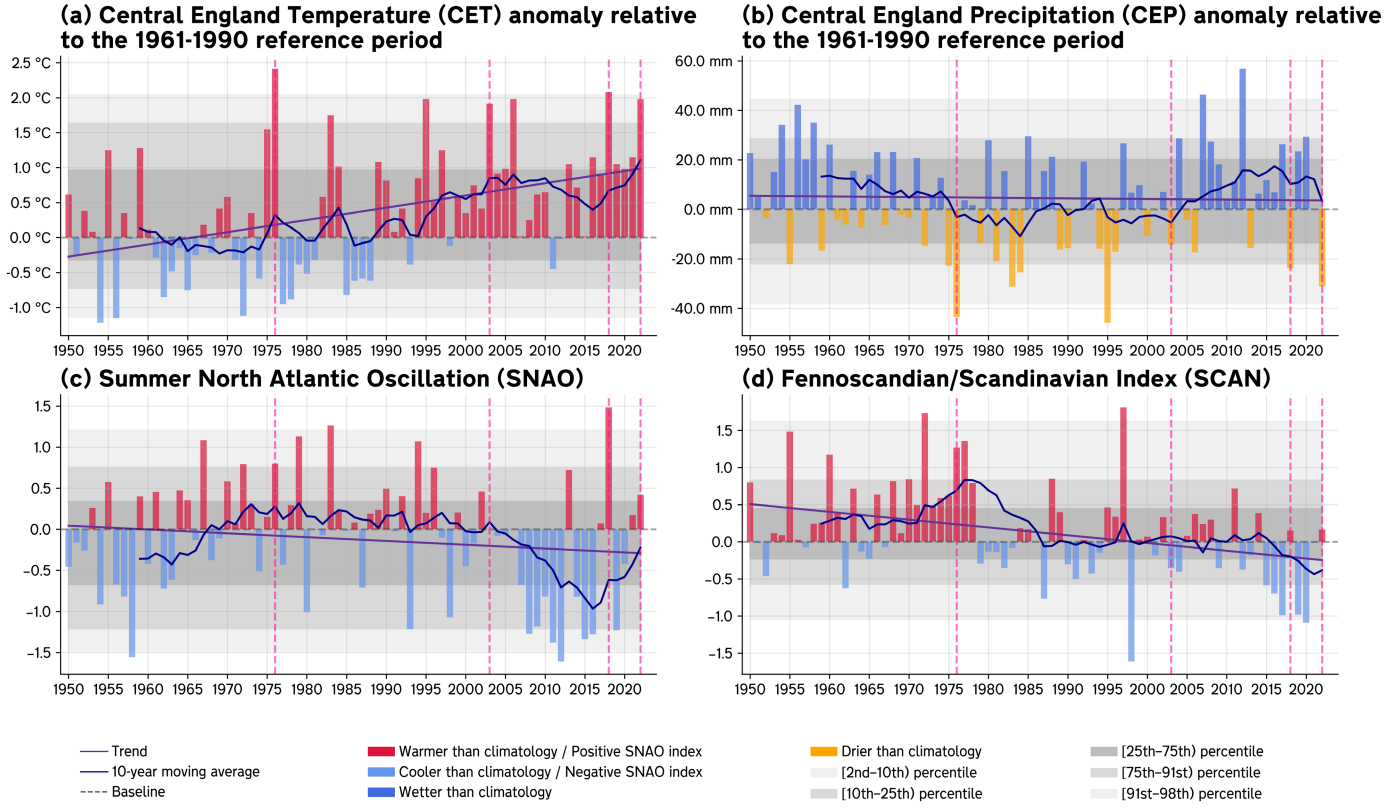

Figure 2. Time series and anomaly trends of all observations and teleconnections analysed (shown as diverging bar plots) – observations: (a) Central England Temperature (CET), (b) Central England Precipitation (CEP); teleconnections: (c) Summer North Atlantic Oscillation (SNAO), (d) Fennoscandian/Scandinavian Index (SCAN). The anomalies are calculated with respect to the 1961–1990 reference period. The solid purple line represents the JJA 1950–2022 linear trend (longer-term variability), while the dark blue line reveals the decadal moving average (shorter-term variability). The vertical dashed lines identify the analysed test cases. The grey and dark grey shading corresponds to the 2nd–98th and 25th–75th percentile rankings, respectively, based on the calculated 1950–2022 observed summer climatology.

SCAN to determine their relationship for the 1950–2022 observed period.

Pearson's correlation and ordinary least square linear regression are used to examine the linear association and relationship between the teleconnection indices (i.e. SNAO and SCAN) and the CET and CEP anomalies. Calculations are performed using pre-built Python scipy. stats package and linregress method that returns the *p*-value from the two-sided *t*-test of the goodness of fit, evaluated at 0.05 significance level. Furthermore, the same test is conducted to examine the exceedance for the prescribed 95th percentile threshold.

Results

We conduct a thorough meteorological and climatological analysis to develop the broader picture between the atmospheric parameters and large-scale drivers (i.e. teleconnections) conducive to heatwave development and amplification. Firstly, the simple statistical analysis estimates the linear relationships between the analysed teleconnections and their relation to the synoptic analysis between the teleconnections and the synoptic analysis (separately evaluating different levels within the atmosphere), unfolding from 200hPa to near-surface level (1000hPa). Later, we associate the weather regimes for the UK with the analysed synoptics. The obtained results provide a quantitative rationale for the case studies' significance and fortify the qualitative findings.

Long-term variability

Building on the qualitative assessment, we statistically examine the role of large-scale drivers of variability. These features interact with the weather systems and influence the strength of the summer heatwaves across the UK.

The CET has a moderate positive correlation with the SNAO+ phase ($r=0.32$), and its peaks coincide with the warmest British summers in the available time series (i.e. 1976, 1983, 1995, 2018, 2022) (Figures 2a, c). *De facto*, the SNAO+ during the summer of 2018 was the highest within the analysed period (see shaded grey confidence regions in Figure 2c), while in the series extending to 1850 was the fourth strongest (McCarthy *et al.*, 2019). Three of the four heatwaves considered exhibit highly positive SNAO and CET, but none of them demonstrate a relationship with SCAN ($r=-0.02$, $p=0.85$).

The CEP shows a strong negative correlation ($r=-0.63$) with the SNAO+ for the analysed test cases and concurs with the precipitation reduction observed during one of the driest summers (Figures 2b, c). However, the dryness signal is less pronounced with the lower correlation magnitude for SCAN+ ($r=-0.14$) due to the Fennoscandian high-pressure magnitude, tilt, and compensatory low-pressure system in the Atlantic, implying that SCAN is not the main driver of the CEP ($p=0.24$).

The calculated *p*-values support the findings, with statistical significance found between the SNAO and CET and SNAO and CEP ($p=0.00$), implying that the CET and CEP are mainly explained by the SNAO variability (Figure 3).

Synoptics

We now delve into the detailed synoptic conditions of various prognostic upper and lower tropospheric variables to relate them to the distinctive properties of the SNAO and their relationship with the CET and CEP. These findings underpin the identification of the local weather regimes conducive to heatwave developments and amplification.

Jet stream

The summer heatwaves of 1976, 2003, 2018 and 2022 all exhibit a 'double jet stream' (Rousi *et al.*, 2022, 2023), characterised by two bands of zonal wind maxima at 200hPa (Figure 4). Anomalously weak westerly winds at 200hPa are observed across the northern Atlantic for the 1976 and 2018 cases (anomalies up to $-10 ms^{-1}$), with two compensating bands of strong zonal wind across the Mediterranean Sea and north of the UK (Figures 4a, c). Similarities between 1976 and 2018 are also found in the regions where zonal wind exceeds two standard deviations: near Iceland and south of the Azores, closer to the northwestern African shores. However, the subtropical jet branch is weaker across the Mediterranean Sea dur-

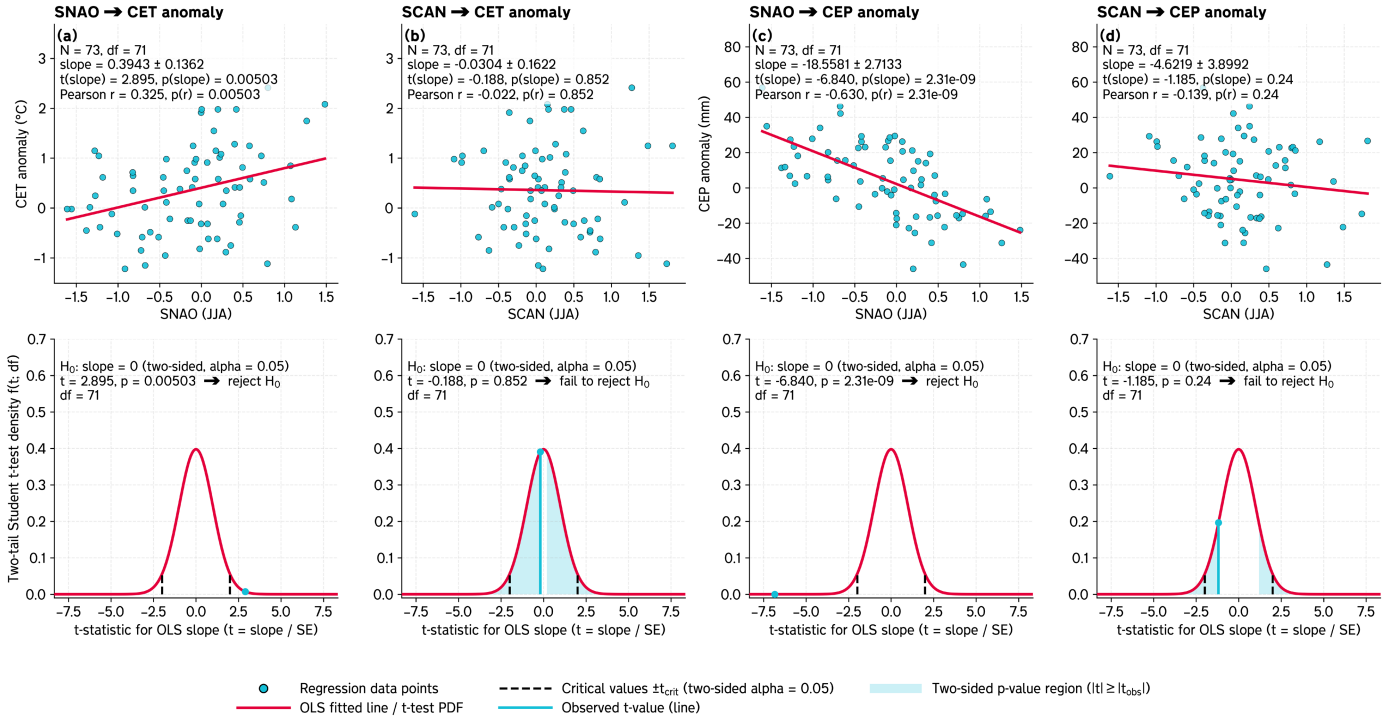

Figure 3. Inferential statistical analysis of the large-scale atmospheric drivers and observations across the 1950–2022 observed period: Pearson correlation (top) and p-value (bottom) obtained as a measure of the two-tailed t-test for goodness of fit at the 0.05 significance level. p-values above 0.05 are considered insignificant. (Source: ERA5, NCEP/NCAR, UK Met Office HadCET and HadUKP (Barnston and Livezey, 1987; Parker et al., 1992; Alexander and Jones, 2000; Hersbach et al., 2020).)

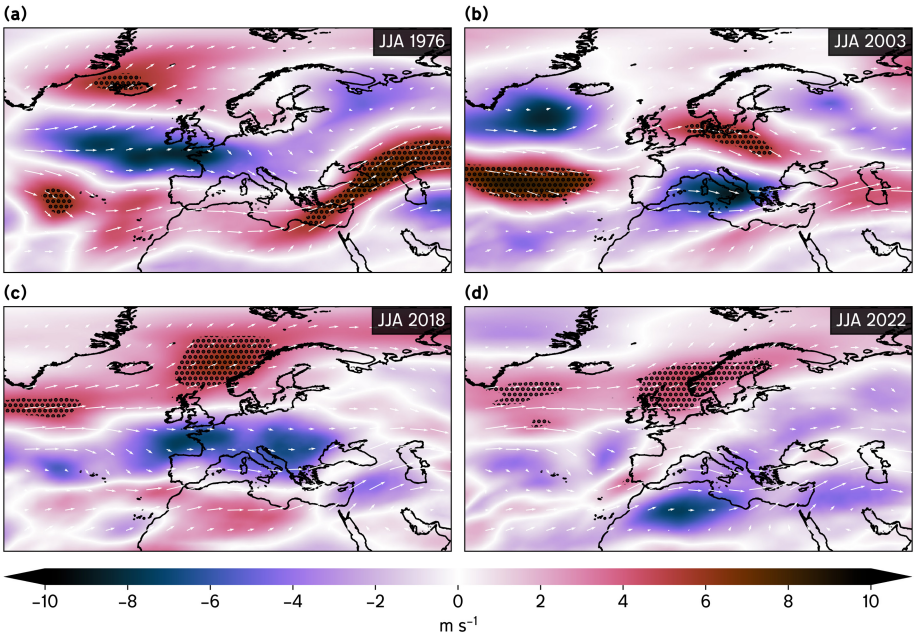

Figure 4. The mean zonal wind anomaly at 200hPa (approximately 10km above the surface) across Europe and the North Atlantic during meteorological summer for the 1961–1990 reference period (in ms^{-1}). Vectors show the zonal wind speed that year while the anomaly is shown with colour shades (from dark reds to dark blues indicating westerlies and easterlies, respectively). Stippling indicates where anomalies for the easterly wind component exceeds the two standard deviations (the 98th percentile category). (a) 1976, (b) 2003, (c) 2018, (d) 2022. (Source: ERA5)

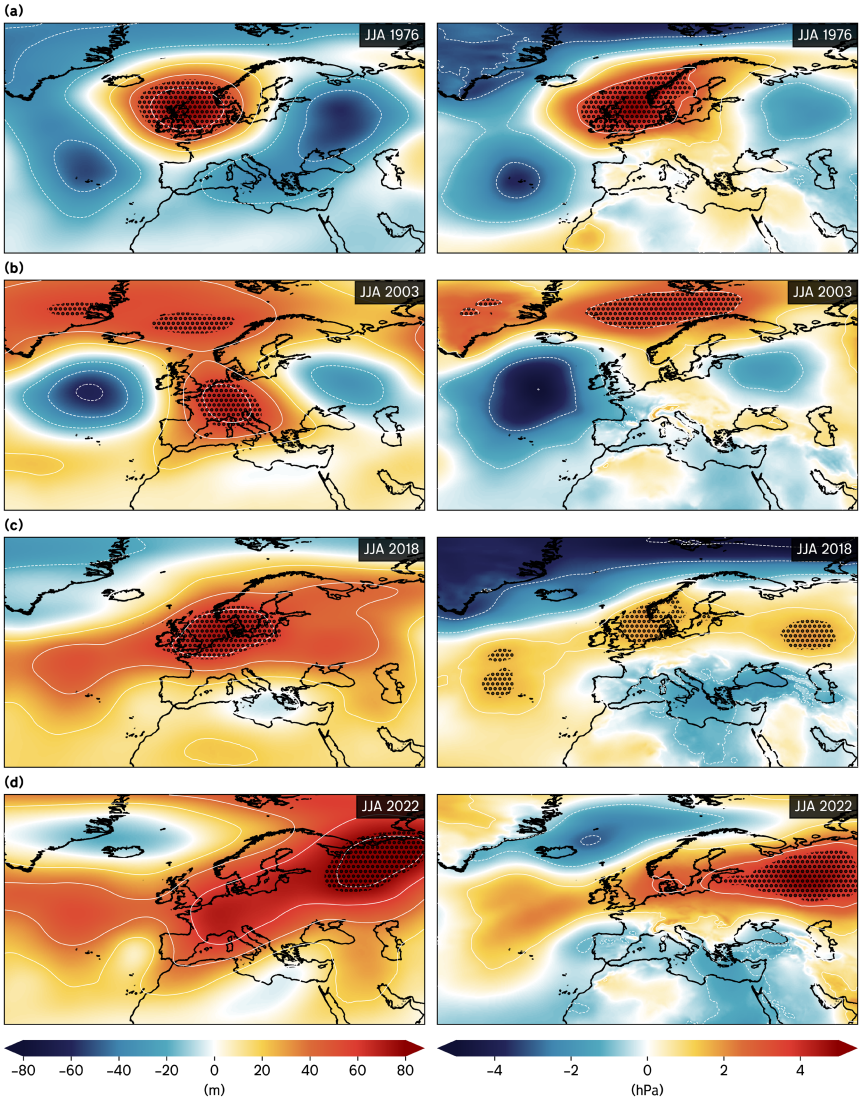

ing the summer of 2018 than in 1976, especially across the eastern Mediterranean Sea, counterbalanced by the stronger easterly air stream across eastern Europe, tilting the high-pressure system to emerge to the east.

In contrast, summer 2003 reveals markedly opposite large-scale atmospheric circulations to the other test cases. The easterly flow is positioned across the western Mediterranean Sea and mainland Europe to the east, and closer to Greenland to the west, with the westerly bands pushed in the central Atlantic and across northern and eastern Europe, elongating the jet stream (Figure 4b). The summer of 2022, meanwhile, blends the influences of the patterns from 1976 and 2018, especially for the anomalously strong easterlies in the northern Atlantic, while the subtropical jet branch shares some similarities with 2003 (Figure 4d).

Geopotential height and mean sea-level pressure

The anomalously strong easterly winds in the upper troposphere during the summer of 1976 and 2018 were conducive to anticyclonic circulation developing, with a robust, persistent high-pressure influence resembling the SNAO+ signature (Figures 5a, c). A stark contrast between these summers is the dominant subtropical ridge extending from north Africa towards central and northern Europe, edging across the southeastern and eastern parts of the UK on the rear flank (Figure 5b). Summer 2018 was dominated by a high-pressure ridge stretching across the North Atlantic towards the British Isles and large parts of northern and central Europe (Figure 5c). However, the anticyclonic tilt in 2018 was closer to Fennoscandia, introducing a more northerly airflow component. This indicates more localised and stronger heatwave influences for the UK in 1976 than in 2018, as the upper-level troughs extended from Greenland to the Azores, and to the east from Eurasia and the Mediterranean, exhibiting the blocking pattern under prevalent dry and hot continental easterly air stream.

Some spatial similarities are also found between 1976 and 2003 in the upper-level troughs to the east and west across the same

Figure 5. The geopotential height anomalies at 500hPa (approximately 5.5km above the surface, left column) and mean sea-level pressure anomalies (right column) across Europe and North Atlantic during meteorological summer with respect to the 1961–1990 reference period. Line contours show the geopotential height anomalies at 20m intervals and mean sea-level pressure on 2hPa intervals, respectively. Colour contours (from dark blues to dark reds) indicate the systems' strength. Stipples indicate where anomalies exceed the two standard deviations (i.e. the 95th percentile category). (a) 1976, (b) 2003, (c) 2018, (d) 2022. (Source: ERA5)

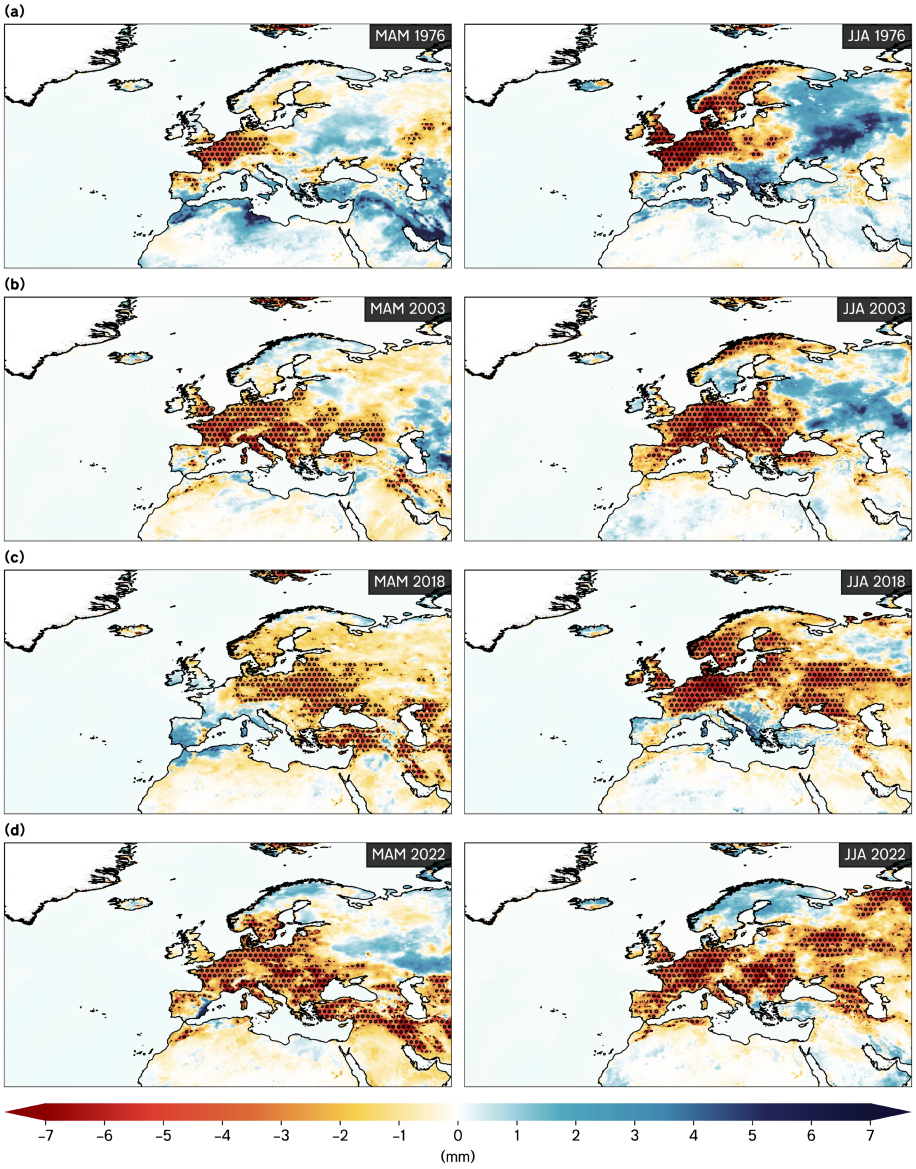

Figure 6. The soil moisture in the first level (i.e. the 0–7cm depth) across Europe and the North Atlantic during meteorological spring and summer (i.e. MAM and JJA seasons) for the 1961–1990 reference period, with stipples indicating anomalies below the two standard deviations (the 95th percentile category). (a) 1976, (b) 2003, (c) 2018, (d) 2022. (Source: ERA5)

regions. Compared to 1976, the Eurasian low position is similar, while the unseasonably deep low-pressure system (anomalies up to −4hPa) was slightly displaced from the Azores to the central Atlantic. It was balanced by a robust upper-level ridge extending northeastwards from North Africa across mainland Europe, merging with the high-pressure system north of Fennoscandia and extending towards Greenland. This allowed a stagnant, blocked pattern throughout the southerly air stream-dominated summer, induced on the rear flank of the high-pressure system across mainland Europe (Figure 5b).

The summer of 2022 blends the influence of the ridge extending from Eurasia eastwards with the mid-Atlantic ridge close to the Portuguese coast. This reinforced prevalent south-southeasterly airflow and a mixture of tropical continental flow from the south, driven by the trough on the front flank and mainland continental air masses from the ridge from the east. It contributed to persistent periods of anomalously hot and dry conditions across the UK, especially during July and August, indicated through the geopotential height anomalies (>50m), resembling the 2003 case (Figures 5b, d).

Note that the 500hPa geopotential height and mean sea-level pressure anomalies in 1976 and 2018 exceed two standard deviations, indicating unusual synoptic conditions over the British Isles and coinciding with the SNAO+ phase, while in 2003 and 2022, mean sea-level pressure anomalies remained within the climatology. This indicates that the heatwave events in 1976 and 2018 were more prolonged than those in 2003 and 2022, which were short but rather intense.

Hence, the most pivotal synoptic conditions coinciding with heatwave developments are upper-level strong easterly wind anomalies in the North Atlantic, which slow down atmospheric dynamics and induce the atmospheric blocking conditions, with a locked-in high-pressure system near the surface. This aligns with the SNAO+-like pattern observed in 1976 and 2018. Furthermore, the ridge-axis tilt (north Africa-Europe in 1976 *vs* North Atlantic-Fennoscandia in 2018) sets the dominant air stream direction and determines the heat localisation, clearly distinguishing the summers with long-lasting heat from shorter, more intense heat episodes.

Antecedent conditions

Soil moisture

In the springs of 1976, 2003, and 2022, soil moisture levels in the uppermost layer of the surface were notably drier than average (i.e. −5 to −10mm) across much of western and northwestern Europe, including the southern parts of the British Isles (Figures 6a, b, and d). In contrast, the spring of 2018 experienced average to slightly wet conditions (Figure 6c). The persistent anticyclonic conditions across northwestern Europe during such summers, especially in 1976, corresponded with long-lasting heatwaves. The Azores high-pressure system during late June and early July 1976 resulted from daily heating and stronger air compression, amplifying the drought effects.

During the spring of 2003, the moisture content at the surface was reduced and drier-than-normal conditions prevailed (Figure 6b). The unseasonably strong low-pressure system and zonal winds in the North Atlantic during summer coincided with the southward-shifted jet stream towards the coast of northwestern Africa, importing a hot and mainly dry air mass across central and northwestern Europe (Figures 4b and 5b). The reduced cloudiness contributed to the diabatic surface heating, with soil moisture substantially below normal (Figure 6b).

The summer of 2018 replicated the anomalies found in 1976, but saw the British Isles experience wetter soils (Figures 5a, 6a and 5c, 6c). However, the enhanced surface heating and prevalently clear skies in late spring set the stage for persistent heatwaves.

In spring 2022, conditions resembled those of 2003, but the negative soil moisture anomalies were more pronounced during summer (Figures 6b, d). A weaker low-pressure system in the North Atlantic and a northward displacement of the Azores high contributed to higher temperatures across the British Isles, marked by continuous adiabatic air compression, warmer SSTs

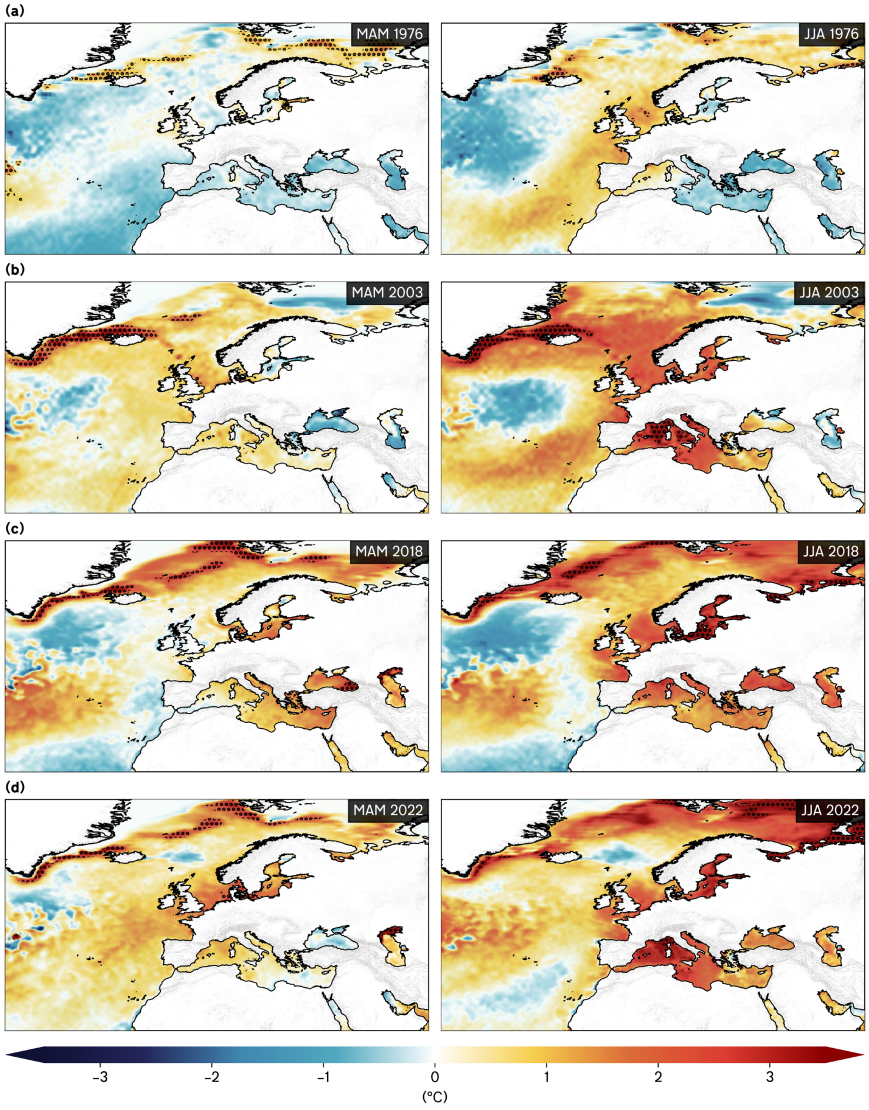

Figure 7. The SST anomalies across Europe and the North Atlantic during meteorological spring and summer for the 1961–1990 reference period. Colour shades (from dark blues to dark reds) show the anomalies, while the stipples indicate where the anomalies exceed the two standard deviations (the 95th percentile category). (a) 1976, (b) 2003, (c) 2018, (d) 2022. (Source: ERA5)

and limited moisture availability, which set the stage for record-breaking heat.

Sea surface temperature

A cool–warm–cool tripole pattern observed during spring is notable in 1976 and 2018 (Figures 7a, c), with cooler-than-normal temperatures across the North Atlantic, while slightly warmer SSTs near Newfoundland indicate weak zonal winds and a northward jet stream (Figure 4a). The anomalies were more pronounced in 2018, likely reflecting an ongoing warming climate and improved satellite data assimilation.

In 1976, stronger anticyclonic influence over the British Isles and its circulation amplified the meridional heat transport, causing stronger sea surface heating and displacing the jet stream poleward (Figures 4a, 5a, and 7a). This phenomenon resulted in reduced soil moisture and lower evaporation rates, thus aiding the formation of a heat dome (Figure 6a).

In contrast, spring 2003 saw a reversed tripole pattern (warm–cool–warm, WCW), with a cold bubble in the central Atlantic and warm temperatures near Greenland, indicating a warm phase of the Atlantic multidecadal variability (Figure 7b). This configuration elongated the jet stream, allowing frequent heat plumes from the south to elevate SSTs towards Greenland (Figures 4b, 5b, and 7b).

The 2022 heatwave exhibited characteristics of both 2003 and 2018, with lingering warm SSTs near UK shores and strong zonal winds similar to 2003 (Figures 4b, d). Cooler temperatures around Greenland corresponded with lower pressure, facilitating heat plumes from north Africa, paralleling the patterns of 2003 while retaining the ridge observed in 2018 (Figure 5b, d). Enhanced marine heatwaves, such as in 2022, have similarly gained recent research interest due to their role in increasing temperatures and altering ocean–atmosphere–land interactions (Guinaldo *et al.*, 2023).

UK Met Office weather regimes

We also analyse the case studies in relation to the UK Met Office 30 weather regimes (Ansell *et al.*, 2006; Neal *et al.*, 2016; Neal, 2022) to assess the leading patterns influencing heatwaves in the UK. For the summers of 1976 and 2018, the primary weather pattern was pattern 6 (i.e. the anticyclonic Azores high extending towards the UK), observed on 18.5% and 17.4% of total summer days, respectively (Figure 8a, c). This pattern resulted in reduced zonal wind flow, leading to positive anomalies in geopotential height and mean sea-level pressure across northwestern Europe with notable easterly to southeasterly air streams. While both summers were dry, 1976 experienced more extreme conditions due to persistent drought that began in spring 1975 (Rodda and Marsh, 2011), alongside the influence of additional patterns (i.e. patterns 12 and 16), which were less prevalent in 2018.

In contrast, summer 2003 saw a significant displacement of the Azores high southward due to stronger zonal winds, which affected heat distribution and led to a cyclonic southwesterly pattern with a returning polar maritime air mass (i.e. pattern 2). In 2022, conditions were similar to 2003, characterised by a northward-displaced Azores high- and a low-pressure system near Portugal, both summers sharing drier-than-average soils (Figure 6b, d) and warmer-than-average SSTs (Figure 7b, d). The summer of 2022 recorded the first 40°C temperature in the UK on the 19 July, attributed to pattern 2 (figure not shown).

Conclusion

A strong negative correlation ($r = -0.63$) exists between the SNAO and the CEP, indicating a robust linear relationship between observed variables. In contrast, weaker positive correlations are observed for SCAN ($r = 0.26$) and CET ($r = 0.32$). Regression analysis confirms significant differences among the groups, attributed to the positions of the Azores high and Icelandic low, which influence the jet stream position. This indicates that the CET and CEP variability is largely influenced by the SNAO index, and broadly consistent with the findings of Rehman *et al.* (2023) on the Azores high influence and its position. The northward shift of the subpolar gyre and the extension of the subtropical high polewards favour the development of a blocking high over Fennoscandia. The block enables a high-pressure system to prevail across the UK, with predominantly dry and sunny conditions associated with

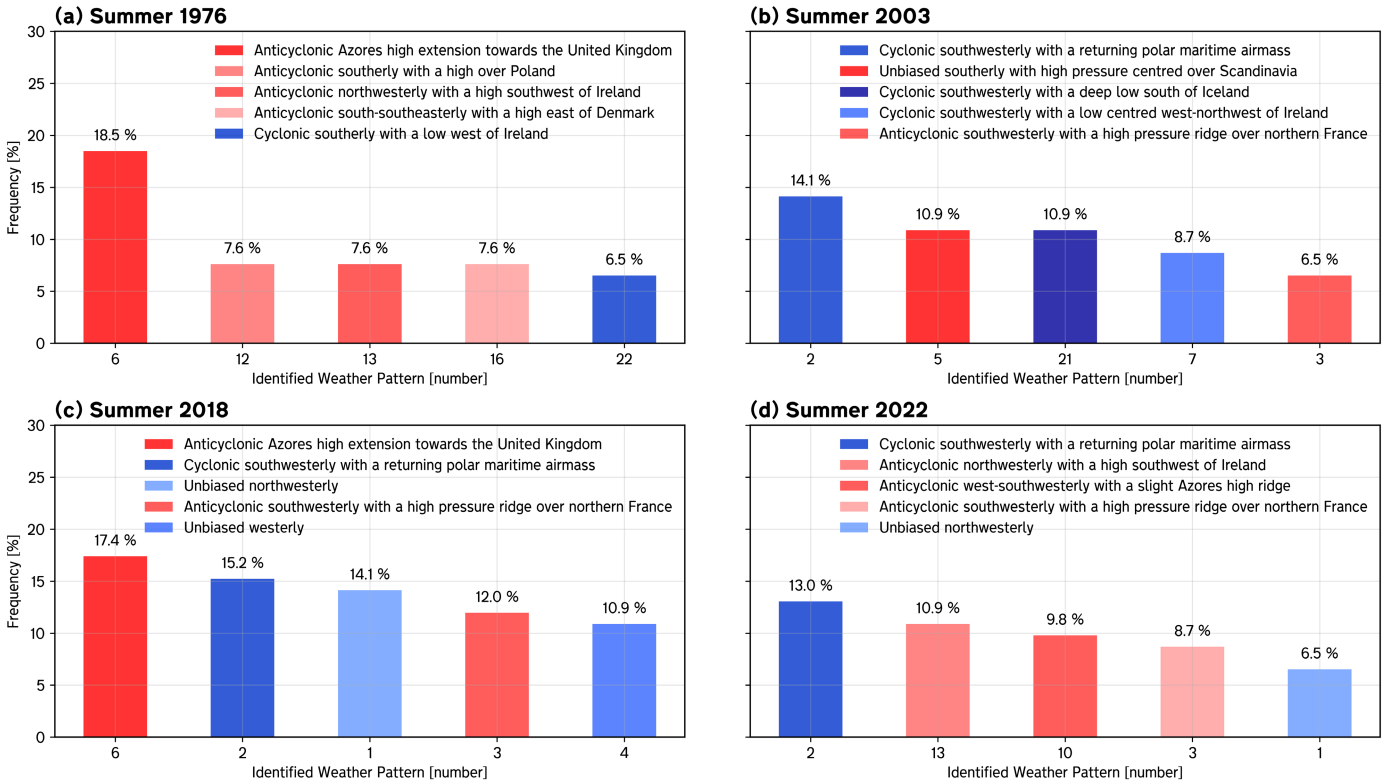

Figure 8. Cumulative seasonal frequency of the Met Office weather patterns/regimes for the selected test cases: (a) 1976, (b) 2003, (c) 2018, (d) 2022. The cyclonic regimes are represented in blue bars while anticyclonic in reds. (Source: UK Met Office (Neal et al., *2016; Neal, 2022))*

the pattern 6 of the MO-30 – or anticyclonic Azores high extension towards the UK ('UK Met Office weather regimes' section). This concurs with the observed lowest CEP climatology values in 1976 and 2018, although the CET experiences variability due to the dominant air stream being influenced by an anticyclonic tilt.

Most analysed summers align with the SNAO+ phase. However, in 2003, an SNAO– summer featured intensely heat-loaded plumes, yielding a CET comparable to SNAO+ summers like 2018 and 2022. Advective processes, in general, play a fundamental role in heatwave developments, with two notable synoptic patterns characterised by the presence of a double jet stream. A blocking signature across Fennoscandia acts as a precursor for prolonged UK heatwaves due to a quasi-stationary high-pressure system drawing warm, dry air from mainland Europe, pushing the jet stream northward, as observed in 1976 and 2018. The difference between these summers lies in the high-pressure system's positioning – over the UK in 1976 *versus* more northeasterly in 2018 – yet both were marked by SNAO+ and anomalously sunny, dry weather conditions.

Alternatively, heatwave developments can result from stronger baroclinicity and deep depressions in the North Atlantic, as seen in 2003 and 2022, which produce intense but short-lived heat plumes moving northward from Iberia and France, contributing to record temperatures. Dry soils amplify heatwave intensities by limiting the energy expended for evaporation, although drought is not found to be a primary precursor. Although sharing similar synoptics with 1976 and 2022, in which coupling effects between land, ocean and atmosphere enhanced heatwave duration, the wetter soils of spring 2018 suppressed this effect. Clear-sky conditions enhance shortwave heating at both the land and ocean surface. At a moisture-limited land interface, the additional daytime energy is increasingly partitioned into sensible rather than latent heat flux, which raises near-surface air temperatures and further dries the land surface, thereby reinforcing the heatwave. Such a feedback mechanism increases solar radiation absorption and atmospheric heating, sustaining hotter and drier near-surface conditions and can amplify heatwave intensity and duration. Over the ocean, weak near-surface winds favour the development of a shallow diurnal warm layer that accumulates heat during the day. This raises the uppermost ocean layer temperature by 3–4°C (Börner *et al.*, 2025) and releases it at night, limiting nocturnal cooling of the overlying air. It is analogous to what was observed in 2003 and 2022, both of which featured marine heatwaves (Guinaldo *et al.*, 2023). The WCW tripole pattern – warmer SSTs near Newfoundland and south of Greenland, and a colder mid-Atlantic belt – also supports hot, dry summers across the UK by altering jet stream dynamics and meridional transport.

This study demonstrates that no single teleconnection or variable results in extreme heatwaves, but a careful consideration of the general weather regime in winter and spring can aid predictive power. The scheme would be refined by examining more marginal heatwaves, and the soil moisture analysis may provide context for small-scale heat events. These heatwaves, such as 1975 (particularly over Denmark and Sweden), 1983, 1995 and 2013 (UK focussed), are thereby limited to specific locations and may differ in spatiotemporal magnitude and extent. Future work following this paper will consider expanding the qualitative findings and applying quantitative methods focussing on the statistical analyses of the interannual variability (e.g. Simmonds and Li, 2021) and trends of the synoptic variables conducive to the heatwave developments and amplification.

Acknowledgements

Richard P. Allan received funding from the National Centre for Earth Observation (NE/RO16518/1, NE/Y006216/1).

Author contributions

Dan Suri: Writing – review and editing; supervision; methodology; conceptualization. **Tim Trent:** Writing – review and editing;

supervision; methodology; conceptualization. **Adam C. Povey:** Writing – review and editing; supervision; methodology; conceptualization. **Richard P. Allan:** Writing – review and editing; supervision; methodology; conceptualization. **Nedim Sladić:** Writing – original draft; writing – review and editing; visualization; methodology; formal analysis; data curation; conceptualization.

Conflict of interest

D. Suri is a member of the *Weather* editorial board but was not privy to the peer review process.

Data availability statement

All the data used for this research is available from the corresponding author upon reasonable request.

References

Alexander L. 2011. Extreme heat rooted in dry soils. *Nat. Geosci.* **4**: 12–13. https://doi.org/10.1038/ngeo1045

Alexander LV, **Jones PD**. 2000. Updated precipitation series for the U.K. and discussion of recent extremes. *Atmos. Sci. Lett.* **1**: 142–150. https://doi.org/10.1006/asle.2000.0016

Ansell TJ, **Jones PD**, **Allan RJ** *et al*. 2006. Daily mean sea level pressure reconstructions for the European–North Atlantic region for the period 1850–2003. *J. Clim.* **19**: 2717–2742. https://doi.org/10.1175/JCLI3775.1

Ballester J, **Quijal-Zamorano M**, **Méndez Turrubiates RF** *et al*. 2023. Author correction: heat-related mortality in Europe during the summer of 2022. *Nat. Med.* **30**(2): 603. https://doi.org/10.1038/s41591-023-02649-1

Barnston AG, **Livezey RE**. 1987. Classifications, seasonality, and persistence of low-frequency atmospheric circulation patterns. *Mon. Weather Rev.* **115**: 1083–1126. https://doi.org/10.1175/1520-0493(1987)115%3C1083:CSAPOL%3E2.0.CO;2

Bell B, **Hersbach H**, **Simmons A** *et al*. 2021. The ERA5 global reanalysis: preliminary extension to 1950. *Q. J. R. Meteorol. Soc.* **147**: 4186–4227. https://doi.org/10.1002/qj.4174

Black E, **Blackburn M**, **Harrison G** *et al*. 2004. Factors contributing to the summer 2003 European heatwave. *Weather* **59**: 217–223. https://doi.org/10.1256/wea.74.04

Börner R, **Haerter JO**, **Fiévet R**. 2025. DiuSST: a conceptual model of diurnal warm layers for idealized atmospheric simulations with interactive sea surface temperature. *Geosci. Model Dev.* **18**: 1333–1356. https://doi.org/10.5194/gmd-18-1333-2025

Brimicombe C, **Porter JJ**, **Di Napoli C** *et al*. 2021. Heatwaves: an invisible risk in UK policy and research. *Environ. Sci. Pol.* **116**: 1–7. https://doi.org/10.1016/j.envsci.2020.10.021

Cassou C, **Terray L**, **Phillips AS**. 2005. Tropical Atlantic influence on European heat waves. *J. Clim.* **18**: 2805–2811. https://doi.org/10.1175/JCLI3506.1

Christidis N, **McCarthy M**, **Stott PA**. 2020. The increasing likelihood of temperatures above 30 to 40°C in the United Kingdom. *Nat. Commun.* **11**: 3093. https://doi.org/10.1038/s41467-020-16834-0

Coumou D, **Di Capua G**, **Vavrus S** *et al*. 2018. The influence of Arctic amplification on mid-latitude summer circulation. *Nat. Commun.* **9**: 2959. https://doi.org/10.1038/s41467-018-05256-8

Cucchi M, **Weedon GP**, **Amici A** *et al*. 2020. WFDE5: bias-adjusted ERA5 reanalysis data for impact studies. *Earth Syst. Sci. Data* **12**: 2097–2120. https://doi.org/10.5194/essd-12-2097-2020

Dickinson N, **Spencer LH**, **Yang S** *et al*. 2025. Extreme weather events in the UK and resulting public health outcomes. *Int. J. Public Health* **70**. https://doi.org/10.3389/ijph.2025.1607904

Dunstone N, **Smith D**, **Hardiman S** *et al*. 2019. Skilful real-time seasonal forecasts of the dry northern European summer 2018. *Geophys. Res. Lett.* **46**: 12368–12376. https://doi.org/10.1029/2019GL084659

Fischer EM, **Seneviratne SI**, **Lüthi D** *et al*. 2007. Contribution of land-atmosphere coupling to recent European summer heat waves. *Geophys. Res. Lett.* **34**: L06707. https://doi.org/10.1029/2006GL029068

Folland CK, **Knight J**, **Linderholm HW** *et al*. 2009. The summer north Atlantic oscillation: past, present, and future. *J. Clim.* **22**: 1082–1103. https://doi.org/10.1175/2008JCLI2459.1

Guinaldo T, **Voldoire A**, **Waldman R** *et al*. 2023. Response of the sea surface temperature to heatwaves during the France 2022 meteorological summer. *Ocean Sci.* **19**: 629–647. https://doi.org/10.5194/os-19-629-2023

Hersbach H, **Bell B**, **Berrisford P** *et al*. 2020. The ERA5 global reanalysis. *Q. J. R. Meteorol. Soc.* **146**: 1999–2049. https://doi.org/10.1002/qj.3803

Hirschi M, **Seneviratne SI**, **Alexandrov V** *et al*. 2011. Observational evidence for soil-moisture impact on hot extremes in southeastern Europe. *Nat. Geosci.* **4**: 17–21. https://doi.org/10.1038/ngeo1032

Howarth C, **Kantenbacher J**, **Guida K** *et al*. 2019. Improving resilience to hot weather in the UK. *Environ. Sci. Pol.* **94**: 258–261. https://doi.org/10.1016/j.envsci.2019.01.008

Hurrell JW. 1995. Decadal trends in the North Atlantic Oscillation. *Science* **269**: 676–679. https://doi.org/10.1126/science.269.5224.676

Johnson H, **Kovats RS**, **McGregor G** *et al*. 2005. The impact of the 2003 heat wave on daily mortality in England and Wales. *Euro Surveill.* **10**: 168–171.

Jones PD, **Jonsson T**, **Wheeler D**. 1997. Extension to the North Atlantic Oscillation using early instrumental pressure observations from Gibraltar and South-West Iceland. *Int. J. Climatol.* **17**(13): 1433–1450. https://doi.org/10.1002/(SICI)1097-0088(19971115)17:13%3C1433::AID-JOC203%3E3.0.CO;2-P

Kornhuber K, **Osprey S**, **Coumou D** *et al*. 2019. Extreme weather events in early summer 2018 connected by a recurrent hemispheric wave-7 pattern. *Environ. Res. Lett.* **14**: 054002. https://doi.org/10.1088/1748-9326/ab13bf

Lowe JA, **Bernie D**, **Bett PE**, *et al*. 2019. UKCP18 science overview report. https://www.metoffice.gov.uk/pub/data/weather/uk/ukcp18/science-reports/UKCP18-Overview-report.pdf.

Luo D, **Luo B**, **Zhang W** *et al*. 2024. Arctic amplification-induced intensification of planetary wave modulational instability: a simplified theory of enhanced large-scale waviness. *Q. J. R. Meteorol. Soc.* **150**: 2888–2905. https://doi.org/10.1002/qj.4740

Luterbacher J, **Dietrich D**, **Xoplaki E** *et al*. 2004. European seasonal and annual temperature variability, trends, and extremes since 1500. *Science* **303**: 1499–1503. https://doi.org/10.1126/science.1093877

Mann ME, **Rahmstorf S**, **Kornhuber K** *et al*. 2017. Influence of anthropogenic climate change on planetary wave resonance. *Sci. Rep.* **7**: 45242. https://doi.org/10.1038/srep45242

McCarthy M *et al*. 2019. Drivers of the UK summer heatwave of 2018. *Weather* **74**: 390–396. https://doi.org/10.1002/wea.3628

Miralles DG, **Gentine P**, **Seneviratne SI** *et al*. 2019. Land-atmospheric feedbacks during droughts and heatwaves: state of the science and current challenges. *Ann. N. Y. Acad. Sci.* **1436**: 19–35. https://doi.org/10.1111/nyas.13912

Miralles DG, **Teuling A**, **van Heerwaarden C** *et al*. 2014. Mega-heatwave temperatures due to soil desiccation and atmospheric heat accumulation. *Nat. Geosci.* **7**: 345–349. https://doi.org/10.1038/ngeo2141

Mistry MN, **Schneider R**, **Masselot P** *et al*. 2022. Comparison of weather station and climate reanalysis data for modelling temperature-related mortality. *Sci. Rep.* **12**: 5178. https://doi.org/10.1038/s41598-022-09049-4

Neal, R. 2022. *Daily historical weather pattern classifications for the UK*, PANGAEA. https://doi.org/10.1594/PANGAEA.942896.

Neal R, **Fereday RC**, **Comer RE**. 2016. A flexible approach to defining weather patterns in weather forecasting over Europe. *Meteorol. Appl.* **23**: 389–400. https://doi.org/10.1002/met.1563

Office for National Statistics and UK Health Security Agency. 2023. Excess mortality during heat-periods: 1 June to 31 August 2022. https://www.ons.gov.uk/peoplepopulationandcommunity/birthsdeathsandmarriages/deaths/articles/excessmortalityduringheatperiods/englandandwales1juneto31august2022. (accessed 01 September 2025).

Parker D, **Horton B**. 2005. Uncertainties in central England temperature 1878-2003 and some improvements to the maximum and minimum series. *Int. J. Climatol.* **25**: 1173–1188. https://doi.org/10.1002/joc.1190

Parker D, **Legg T**, **Folland C**. 1992. A new daily central England temperature series, 1772–1991. *Int. J. Climatol.* **12**: 317–342. https://doi.org/10.1002/joc.3370120402

Pfahl S, **Wernli H**. 2012. Quantifying the relevance of atmospheric blocking for temperature extremes in the Northern Hemisphere. *Geophys. Res. Lett.* **39**. https://doi.org/10.1029/2012GL052261

Quesada B, **Vautard R**, **Yiou P** *et al*. 2012. Asymmetric European summer heat predictability from wet and dry southern winters and springs. *Nat. Clim. Chang.* **2**: 736–741. https://doi.org/10.1038/nclimate1536

Rehman S, **Usmani BA**, **Simmonds I**. 2023. The separate roles played by the two geographical poles of the NAO in influencing winter precipitation over Spain. *J. Atmos. Sol.-Terres. Phys.* **245**: 106054. https://doi.org/10.1016/j.jastp.2023.106054

Rodda JC, **Marsh TJ**. 2011. The 1975–76 Drought – A Contemporary and Retrospective Review. NERC/Centre for Ecology & Hydrology: Wallingford, UK, pp 1–58.

Rouges E, **Ferranti L**, **Kantz H** *et al*. 2023. European heatwaves: link to large-scale circulation patterns. *Int. J. Climatol.* **43**: 3189–3209. https://doi.org/10.1002/joc.8024

Rousi E, **Fink AH**, **Andersen LS** *et al*. 2023. The extremely hot and dry 2018 summer in central and northern Europe. *Nat. Hazards Earth Syst. Sci.* **23**: 1699–1718. https://doi.org/10.5194/nhess-23-1699-2023

Rousi E, **Kornhuber K**, **Beobide-Arsuaga G** *et al*. 2022. Accelerated western European heatwave trends linked to persistent double jets over Eurasia. *Nat. Commun.* **13**: 3851. https://doi.org/10.1038/s41467-022-31432-y

Rudeva I, **Simmonds I**. 2021. Midlatitude winter extreme temperature events and connections with anomalies in the Arctic and Tropics. *J. Clim.* **34**: 3733–3749. https://doi.org/10.1175/jcli-d-20-0371.1

Sahani J, **Kumar P**, **Debele S** *et al*. 2022. Heat risk of mortality in two different regions of the United Kingdom. *Sustain. Cities Soc.* **80**: 103758. https://doi.org/10.1016/j.scs.2022.103758

Schär C, **Vidale P**, **Lüthi D** *et al*. 2004. The role of increasing temperature variability in European summer heatwaves. *Nature* **427**: 332–336. https://doi.org/10.1038/nature02300

Simmonds I, **Li M**. 2021. Trends and variability in polar sea ice, global atmospheric circulations, and baroclinicity. *Ann. N. Y. Acad. Sci.* **1504**(1): 167–186. https://pubmed.ncbi.nlm.nih.gov/34313329/ (accessed 11 February 2026).

Stéfanon M, **Drobinski P**, **d'Andrea F** *et al*. 2012. Effects of interactive vegetation phenology on the 2003 summer heat waves. *J. Geophys. Res.* **117**: D24103. https://doi.org/10.1029/2012JD018187

Stott P, **Stone DA**, **Allen MR**. 2004. Human contribution to the European heatwave of 2003. *Nature* **432**(7017): 610–614. https://doi.org/10.1038/nature03089

Strigunova I, **Blender R**, **Lunkeit F** *et al*. 2022. Signatures of Eurasian heat waves in global Rossby wave spectra. *Weather Clim. Dynam.* **3**: 1399–1414. https://doi.org/10.5194/wcd-3-1399-2022

Tyrlis E, **Hoskins BJ**. 2008. Aspects of a Northern Hemisphere atmospheric blocking climatology. *J. Atmos. Sci.* **65**: 1638–1652. https://doi.org/10.1175/2007JAS2337.1

Velikou K *et al*. 2022. Reliability of the ERA5 in replicating mean and extreme temperatures across Europe. *Water* **14**: 543. https://doi.org/10.3390/w14040543

Yule EL, **Hegerl G**, **Schurer A** *et al*. 2023. Using early extremes to place the 2022 UK heat waves into historical context. *Atmos. Sci. Lett.* **24**(7). https://doi.org/10.1002/asl.1159

Zschenderlein P, **Fink AH**, **Pfahl S** *et al*. 2019. Processes determining heat waves across different European climates. *Q. J. R. Meteorol. Soc.* **145**: 2973–2989. https://doi.org/10.1002/qj.3599

Correspondence to: N. Sladić
ns654@leicester.ac.uk

doi: 10.1002/wea.70075